Megawatt Pulses from an All-Fiber and Self-Starting Femtosecond Oscillator

HENRY HAIG[1,*], PAVEL SIDORENKO[1], ROBERT THORNE[2,3], AND FRANK WISE[1]

[1] School of Applied and Engineering Physics, Cornell University, Ithaca, New York 14853, USA
[2] Department of Physics, Cornell University, Ithaca, New York 14853, USA
[3] MiTeGen LLC, Ithaca, New York 14852, USA
[*] Corresponding author: tsh67@cornell.edu

Compiled December 18, 2021

Mamyshev oscillators produce high-performance pulses, but technical and practical issues render them unsuitable for widespread use. Here we present a Mamyshev oscillator with several key design features that enable self-starting operation and unprecedented performance and simplicity from an all-fiber laser. The laser generates 110-nJ pulses that compress to 40-fs and 80-nJ with a grating pair. The pulse energy and duration are both the best achieved by a femtosecond all-fiber laser to date, and the resulting peak power of 1.5-MW is 20 times higher than that of prior all-fiber, self-starting lasers. The simplicity of the design, ease of use, and pulse performance make this laser an attractive tool for practical applications.

http://dx.doi.org/10.1364/ao.XX.XXXXXX

Demand for robust ultrafast light sources is increasing as medical, industrial, and scientific communities find new applications for femtosecond pulses. These include surgery [1], protein crystallography [2, 3], micro-machining [4], and biomedical imaging [5]. Mode-locked fiber lasers are good candidates for these applications for several reasons, including their excellent efficiency and beam quality. All-fiber designs with polarization-maintaining (PM) fiber are especially well-suited for commonplace use because they require no alignment, have small physical dimensions, and are environmentally stable. Yet, the fiber format poses challenges: strong nonlinear processes in fiber ultimately limit the achievable pulse energy from fiber lasers. A primary goal of fiber laser research is to build high-performance lasers that also realize the practical advantages of fiber.

Mamyshev oscillators (MOs) have been identified as candidates to realize high-energy, all-fiber lasers [6–8]. These lasers use an effective saturable absorber mechanism that can stabilize highly nonlinear pulse evolutions. Two offset spectral filters in the cavity prevent continuous-wave (CW) lasing but allow pulses that undergo nonlinear spectral broadening between the filters to traverse the cavity. MOs with large mode-area fibers [9] and photonic crystal fibers [10] achieve pulse energies on the microjoule scale, which is an order-of-magnitude improvement over fiber lasers with other saturable absorbers. Typically, MOs are environmentally-stable owing to the use of PM fiber. Fiber-integrated [11–14] or Bragg-grating [15] spectral filters allow construction of all-fiber, compact, and alignment-free MOs.

However, the Mamyshev mechanism presents technical challenges that result in impractical, complex, and costly oscillator designs. Since MO cavities are not resonant, MOs generally do not self-start. A recently-discovered dissipative Faraday instability has been demonstrated to allow self-starting operation of MOs designed to operate with low (picojoule) pulse energies, usually in the harmonic model-locking regime [16, 17]. Most high-energy MOs require a picosecond or femtosecond seed pulse from an additional oscillator to initiate pulsation, which is highly undesirable in a practical instrument [9, 10, 13, 14, 18]. Other designs initiate mode-locking by modulation of the pump power, which can be electronically automated for a "push-button" start [12, 19, 20]. However, in previous designs this method requires additional manipulation of the cavity to reach single-pulse states, which diminishes the viability of this approach for applications that require the most robust operation. The Mamyshev mechanism requires the pulse to broaden spectrally between the offset spectral filters. Some MO designs accomplish this in a ring-type cavity with two gain segments and outputs between the filters, which can be inefficient and costly. Linear-type cavities use a single gain segment, but have not been capable of reaching pulse energies near those of ring-type MOs [20]. While some designs achieve self-starting operation, high-performance, *or* fiber integration, none has all of these features.

The issues discussed above are a significant barrier to the widespread use of Mamyshev oscillators as practical tools. This is reflected in the large gap between the performance of Mamyshev oscillators demonstrated in laser research labs (>100-nJ and <100-fs pulses [9, 10, 14, 21]) and the best performance of a self-starting all-fiber laser (15-nJ and 150-fs pulses [19, 22, 23]) reported to date. All-fiber, self-starting designs will be necessary to realize the performance advantages of MOs for practical applications.

Here we present an all-PM-fiber Mamyshev oscillator with several unique design features, which together result in unprecedented simplicity, ease-of-use, and pulse performance from an all-fiber laser. This is the first experimental demonstration of a ring MO with a passive arm, although this possibility was envisioned in early work [24]. Tuning of the spectral filter pa-

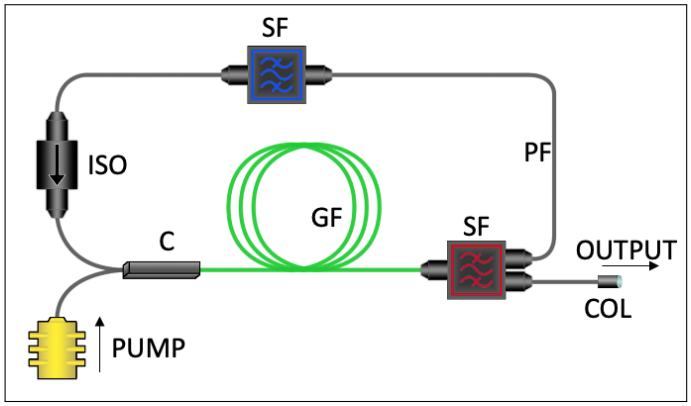

Fig. 1. Schematic of the all-fiber Mamyshev oscillator. ISO, isolator; C, combiner; GF, gain fiber; SF, spectral filter; COL, collimator; PF, passive fiber.

rameters during construction allows the laser to start reliably to single-pulse mode-locked states with pump modulation and no cavity adjustment on each start. The cavity parameters are optimized to accommodate a gain-managed nonlinear amplification (GMNA) evolution [25], resulting in 110-nJ pulses that compress to 40 fs outside the cavity and reach a peak power over 1.5 MW. This peak power exceeds the highest peak-power from an all-fiber, self-starting laser by a factor of 20 [19]. Additionally, these are the highest-energy and shortest-duration pulses from a femtosecond all-fiber oscillator of any kind [14], to our knowledge. The laser's environmental stability, ease of starting, and performance make it very well-suited for practical applications.

A schematic of the oscillator is shown in Fig. 1. The laser is constructed from 9 m of PM fiber and fiber-integrated components. All passive sections and fiber-integrated components use fiber with 8.5-µm core diameter (PM-1060). The active arm has 4 m of co-directionally cladding-pumped active fiber (YB1200-10/125DC-PM) with 10-µm core diameter. The spectral filter following the active arm has 5-nm full-width-at-half-maximum (FWHM) bandwidth centered at 1040 nm, and the filter following the passive arm has 3-nm FWHM bandwidth centered at 1036 nm. Both filters have super-Gaussian transmission profiles.

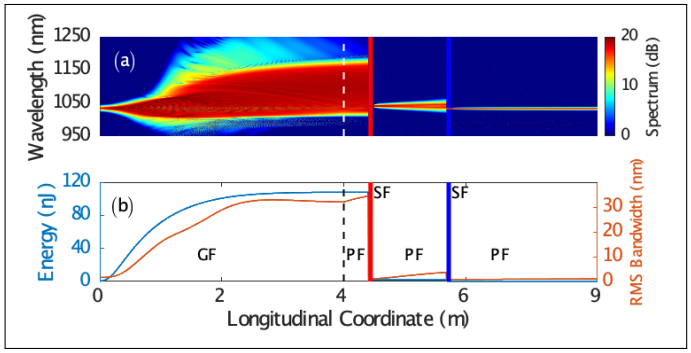

Fig. 2. Simulated evolution of the pulse through the cavity with longitudinal coordinate. (a) shows spectral evolution, (b) shows energy (blue) and root-mean-square (RMS) bandwidth (orange) evolution. The first 4 m of the cavity is gain fiber (GF), and the rest of the cavity is passive fiber (PF). Red and blue lines indicate spectral filters (SF).

Numerical simulations that solve the nonlinear Schrodinger equation guided the design of the laser [26]. The simulations include Kerr and Raman nonlinearities, self-steepening, and up to fourth-order dispersion. The Yb gain spectrum is modeled with steady-state solutions of the rate equations [27, 28]. The model cavity is seeded with a 1 nJ, 1 ps Gaussian pulse with 1040 nm center wavelength which evolves towards a steady-state solution of the cavity over several round trips. The simulated steady-state pulse evolution in the cavity is shown in Fig. 2. Measurements of the pulse (presented below) agree well with simulations. In the active arm the pulse experiences gain and the energy exceeds 100 nJ. The spectrum broadens to well beyond the gain bandwidth of Yb, which is one indication of evolution in the GMNA regime [25]. In this regime, the gain and pulse spectra co-evolve, and the resultant high-bandwidth pulses are compressible to near the transform limit despite very large (> 100 π) nonlinear phase accumulation. After amplification, the pulse is spectrally filtered, and several nanojoules pass the filter to propagate through the passive arm. Self-phase-modulation (SPM) causes the spectrum to broaden sufficiently to reach the pass-band of the second filter and complete a cavity round-trip.

The particular formats of the fiber-integrated spectral filters used here have significant impact on the starting capability. Center-wavelength separation between the offset spectral filters is a key parameter to control the state and starting dynamics of Mamyshev oscillators [7, 12, 17, 20]. This parameter controls the effective saturable absorption of the Mamyshev mechanism; larger filter separation corresponds to a saturable absorber with greater saturation power [24, 29]. Accordingly, large filter separation yields high-power, single-pulse states, while smaller separation can result in multi-pulsing. However, several studies have observed that to start an MO with pump modulation, the filter separation must be small enough to permit a small CW component prior to pump modulation and mode-locking [12, 20]. This can result in starting to a multi-pulse or low-energy state, where further increase of the spectral filter separation is required to reach a single-pulse state.

In our laser, starting with pump modulation is achieved by control of the spectral filter parameters. The spectral filter following the passive arm has adjustable center-wavelength and bandwidth. While initially constructing the laser, the center wavelength is adjusted to give the maximum separation from the other filter's center (4 nm) that still accommodates a small CW signal. After initial adjustment, these filter settings are not changed. The laser starts with near-perfect reliability to single-pulse states by modulation of the pump power alone. Specifically, we use a simple function generator to create a 70 kHz [20] square wave signal that drives the pump power between 0 and 8 W. Immediately after the modulation starts, a pulse train that is modulated by the pump signal appears on the photodiode trace. When the pump modulation is turned off, the pump power remains at a constant nonzero value and the laser remains mode-locked. The energy of the starting state can be chosen by the value of the steady-state pump power (4 - 6 W), and can be adjusted after starting without loss of mode-locking or appearance of multi-pulsing. Although we have not performed rigorous starting trials, we have succeeded in starting the laser hundreds of times with this method without failure. In addition, we have achieved this single-pulse self-starting in many different cavity iterations with different spectral filters, which indicates that these conditions are easily repeatable.

As the pulse energy increases, the spectrum broadens and shifts to longer wavelengths, and the dechirped pulse compresses to shorter durations. This behavior and the broad spectra

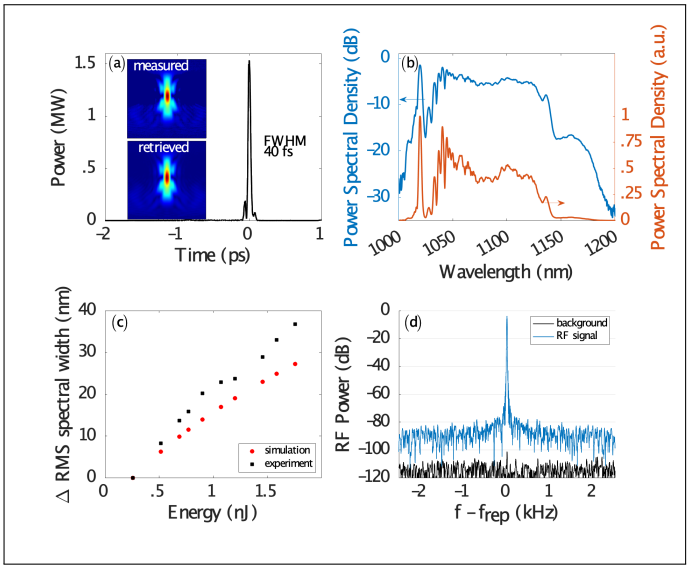

Fig. 3. (a) Compressed pulse measured by frequency-resolved optical gating (FROG). Insets show measured and retrieved FROG traces. (b) Measured spectra in logarithmic (blue) and linear (orange) scale. (c) Peak-power test comparing relative spectral broadening of fractions of the pulse coupled into 1 m of Hi1060 fiber (black) to simulated propagation of gaussian pulses of the same energy and initial bandwidth through the same fiber (red). (d) RF spectrum at the cavity fundamental repetition rate (23.3 MHz) showing signal (blue) and background (black).

observed are consistent with those of other MOs and the trends of the GMNA regime [21, 25]. At 110 nJ, a Raman scattering contribution becomes appreciable (∼ 2% of the pulse energy) above 1150 nm. Increasing the pump power beyond this does not lead to multi-pulsing nor loss of mode-locking, even at the highest output powers we have observed (3 W). However, above 110 nJ, the peak power of the compressed pulse does not increase with pulse energy, as the Raman contribution grows.

A high-performance mode-locked state is summarized in Fig. 3. The laser generates 110-nJ and 4-ps chirped pulses at 23-MHz repetition rate, for an average power of 2.5 W. These are dechirped with a grating pair to yield 80-nJ and 40-fs pulses, with an average power of 1.8 W. The peak power is approximately 1.5 MW. The power scale in Fig. 3(a) is calculated using the energy of the pulse after the compressor. To validate this scale and rule out the presence of either a large pedestal or CW component, we couple a fraction of the compressed pulse into single-mode fiber and compare the measured spectral broadening to that of simulated propagation of a Gaussian pulse with the same initial energy and RMS bandwidth (Fig 3 (c)). Small discrepancies exist between simulated and measured bandwidths, but the trend indicates that the power scale in Fig. 3(a) is valid. The pulse has a small amount of pedestal structure which we estimate to comprise less than 10 % of the pulse energy. Deviation of the pulse from its transform-limited duration (27 fs) is a result of nonlinear phase accumulation and higher-order dispersion during evolution within the cavity. The RF spectrum (Fig. 3(d)) indicates stable mode-locking at the fundamental cavity repetition rate, with contrast between the fundamental frequency and secondary modulations of 80 dB.

Both the high pulse energy and the design with one passive arm are enabled in part by using a filter with a rejection port after the active arm. The spectral components that the filter passes remain in the cavity, while the rejected components form the output pulse. Compared to outputting a fraction of the pulse before filtering, this configuration yields the maximum energy for both the output and recirculating pulses. This enables the use of a passive arm: the pulse entering the passive arm has sufficient peak power to spectrally-broaden adequately. Immediately after the filter, the broad output spectrum is near-zero for wavelengths within the filter passband. However, SPM during propagation of the output pulse through a short (20 cm) fiber pigtail regenerates these spectral components. This explains why the measured spectrum shown in Fig. 3 has nonzero amplitude for wavelengths within the spectral filter passband. Notably, neither this output coupling method nor propagation of the pulse through a short fiber pigtail have significant effect on the compressibility of the pulse with a standard grating compressor. Simulations (data not shown) show that the peak power of the compressed output pulse is within 10 % of the peak-power of the compressed pulse before output coupling.

The fiber lengths have a significant effect on the output pulse parameters, and are tailored to achieve output pulses with the highest peak power. Specifically, the lengths are chosen to promote evolution in the GMNA regime in the active arm. This requires the use of long gain fiber (4 m) with high gain (> 20 dB), and control of the parameters of the pulse that enters the active arm. These parameters are determined primarily by propagation and spectral filtering in the passive arm. The passive arm must be sufficiently long to allow adequate spectral broadening, but we find that using the shortest possible length (1.5 m) that satisfies this requirement produces a pulse with nearly ideal parameters (∼ 1 nJ, ∼ 1 ps, gaussian-like transform-limited spectrum) to seed the GMNA evolution [25]. Simulations and experiments show that a longer passive arm delivers a pulse to the active arm with additional linear and nonlinear phase structure that results in an amplified pulse of lower quality.

The performance of the laser described here is comparable to the best achieved previously with 10-μm fiber [21]; only a factor of 2 in peak power has been sacrificed by the all-fiber design and passive arm. It may be possible to exceed the performance described here by well-known techniques, such as the use of larger-core-diameter fiber. This could potentially lead to all-fiber lasers with microjoule-scale pulse energy. However, it is known that the GMNA evolution is ultimately limited by Raman scattering [25], which we also observe here. Design of fiber lasers that exceed the performance limits of the GMNA evolution will require other techniques, or new insight into nonlinear pulse evolutions beyond the GMNA regime.

In addition to the excellent pulse parameters and reliable self-starting operation, the laser is already a practical instrument. For high-power mode-locked states, the efficiency is over 40%: the 2.6 W output power is achieved with 5.7 W of pump power. As expected with the PM fiber design, operation is impervious to mechanical or thermal perturbations. As a longer-term stability test, we recorded the spectrum and average power each minute for 60 hours (Fig. 4). Over that period, the RMS spectral bandwidth has a standard deviation of 0.25 nm, and the standard deviation of the output power is less than 1 mW (which corresponds to ∼0.5 % relative variation). This power fluctuation is within the uncertainty (± 3%) of the measurement, and illustrates the excellent stability of the laser. In addition, we never observe spontaneous loss of mode-locking.

The small filter separation (4 nm) in this laser is advanta-

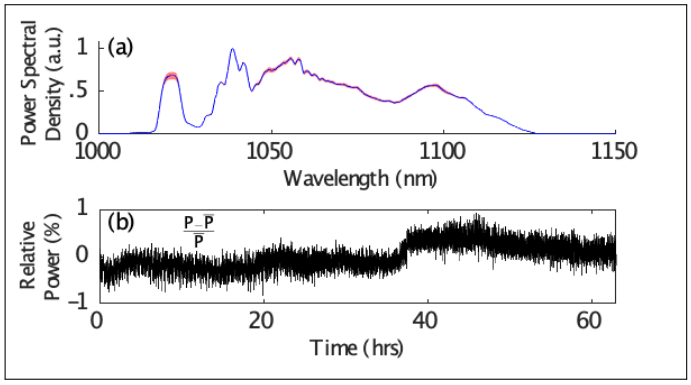

Fig. 4. Stability test (a) Solid blue line shows spectrum averaged over 60 hours. Shaded area in red shows the standard deviation of each spectral component over that timeframe. Linear scale. (b) Change in output power relative to the mean of the output power for 60 hours.

geous because it permits a small CW component and allows self-starting. It is somewhat surprising that the laser operates only in single-pulse states, since previous high-energy Mamyshev oscillators use much larger filter separations (20 nm) [9, 21]). We suspect that the passive arm design may encourage single-pulse operation. Currently, we do not have conclusive evidence to support this claim aside from our observations of single-pulse states, and provide only a speculative explanation. Considering pulses of the same initial shape and chirp, a Mamyshev regenerator will only pass pulses that have peak power above some threshold. This results in the step-function-like saturable absorber curve of Mamyshev oscillators [24]. Because gain generally enhances spectral broadening, the threshold peak power is greater for a passive Mamyshev regenerator than one with gain. This implies that an oscillator with a passive arm has an effective saturable absorption with higher saturation power than one with two active arms. The use of a passive arm would then have a similar effect on the saturable absorption as increased filter separation. This would enable single-pulse operation even with small filter separation, as we observe. Further work will be necessary to understand how the saturable absorption of Mamyshev oscillators is affected by passive propagation.

In conclusion, we have demonstrated a high-performance all-fiber Mamyshev oscillator with unprecedented simplicity and ease-of-starting. The design features a passive arm which simplifies construction and reduces cost. Specific formats of fiber-integrated spectral filters provide maximal output coupling and allow the oscillator to start reliably to single-pulse states by initial modulation of the pump power alone. The pulse evolution is optimized, resulting in generation of pulses that compress to 40 fs and reach 1.5 MW peak power. These parameters are comparable to the highest-performance fiber lasers with free-space elements, which represents a new milestone for fully fiber-integrated designs. The simplicity of use, environmental stability, and pulse performance make this laser well-suited to applications that require megawatt-level femtosecond pulses.

1. BACKMATTER

Acknowledgments. The authors would like to thank Michael Buttolph for helpful discussions related to this work.

Disclosures. HH (P), PS (P), FW (P).

Funding. Portions of this work were supported by the U.S. Department of Energy (DE-SC0019546), the National Institutes of Health (EB002019), and the National Science Foundation (ECCS-1912742).

REFERENCES

1. J. D. Steinmeyer, C. L. Gilleland, C. Pardo-Martin, M. Angel, C. B. Rohde, M. A. Scott, and M. F. Yanik, Nat. Protoc. **5**, 395 (2010).
2. L. M. Haupert and G. J. Simpson, Methods **55**, 379 (2011).
3. H.-Y. Chung, R. Schubert, S.-H. Chia, S. Falke, C. N. Mudogo, F. X. Kärtner, G. Chang, C. Betzel *et al.*, Commun. Biol. **3**, 1 (2020).
4. R. R. Gattass and E. Mazur, Nat. Photonics **2**, 219 (2008).
5. C. Xu and F. Wise, Nat. Photonics **7**, 875 (2013).
6. M. Piche, *Mode locking through nonlinear frequency broadening and spectral filtering*, vol. 2041 (SPIE, 1994).
7. K. Sun, M. Rochette, and L. R. Chen, Opt. Express **17**, 10419 (2009).
8. K. Regelskis, J. Želudevičius, K. Viskontas, and G. Račiukaitis, Opt. Lett. **40**, 5255 (2015).
9. D. Lin, D. Xu, J. He, Y. Feng, Z. Ren, and D. J. Richardson, "Generation of 625nj pulses from a mamyshev oscillator with a few-mode lma yb-doped fiber," in *2021 Conference on Lasers and Electro-Optics Europe and European Quantum Electronics Conference,* (Optical Society of America, 2021).
10. W. Liu, R. Liao, J. Zhao, J. Cui, Y. Song, C. Wang, and M. Hu, Optica **6**, 194 (2019).
11. E. Poeydebat, F. Scol, O. Vanvincq, G. Bouwmans, and E. Hugonnot, Opt. Lett. **45**, 1395 (2020).
12. E. Poeydebat, F. Scol, O. Vanvincq, G. Bouwmans, and E. Hugonnot, "Pulse energy enhancement via filter shape optimization in an all-fiber mamyshev oscillator," in *Conference on Lasers and Electro-Optics,* (Optical Society of America, 2021), p. JTh3A.97.
13. B. Piechal, J. Szczepanek, T. M. Kardaś, and Y. Stepanenko, J. Light. Technol. **39**, 574 (2021).
14. T. Wang, B. Ren, C. Li, J. Wu, R. Su, P. Ma, Z.-C. Luo, and P. Zhou, IEEE J. Sel. Top. Quantum Electron. **27**, 1 (2021).
15. V. Boulanger, M. Olivier, F. Trépanier, M. Bernier, and M. Piché, "Efficient all-pm-fiber mamyshev oscillator based on fiber bragg gratings," in *Laser Congress 2020 (ASSL, LAC),* (Optical Society of America, 2020), p. JTu5A.6.
16. N. Tarasov, A. M. Perego, D. V. Churkin, K. Staliunas, and S. K. Turitsyn, Nat. Commun. **7** (2016).
17. A. M. Perego, Opt. Lett. **42**, 3574 (2017).
18. Z. Liu, Z. M. Ziegler, L. G. Wright, and F. W. Wise, Optica **4**, 649 (2017).
19. I. Samartsev, A. Bordenyuk, and V. Gapontsev, "Environmentally stable seed source for high power ultrafast laser," in *Components and Packaging for Laser Systems III,* , vol. 10085 A. L. Glebov and P. O. Leisher, eds., International Society for Optics and Photonics (SPIE, 2017), pp. 201 – 209.
20. Y.-H. Chen, P. Sidorenko, R. Thorne, and F. Wise, J. Opt. Soc. Am. B **38**, 743 (2021).
21. P. Sidorenko, W. Fu, L. G. Wright, M. Olivier, and F. W. Wise, Opt. Lett. **43**, 2672 (2018).
22. M. Pielach, B. Piechal, J. Szczepanek, P. Kabaciński, and Y. Stepanenko, IEEE Access **8**, 145087 (2020).
23. C. Aguergaray, N. G. R. Broderick, M. Erkintalo, J. S. Y. Chen, and V. Kruglov, Opt. Express **20**, 10545 (2012).
24. S. Pitois, C. Finot, L. Provost, and D. J. Richardson, J. Opt. Soc. Am. B **25**, 1537 (2008).
25. P. Sidorenko, W. Fu, and F. Wise, Optica **6**, 1328 (2019).
26. G. P. Agrawal, *Nonlinear Fiber Optics* (Academic Press, 1995), 2nd ed.
27. S. K. Turitsyn, A. E. Bednyakova, M. P. Fedoruk, A. I. Latkin, A. A. Fotiadi, A. S. Kurkov, and E. Sholokhov, Opt. Express **19**, 8394 (2011).
28. R. Paschotta, J. Nilsson, A. Tropper, and D. Hanna, IEEE J. Quantum Electron. **33**, 1049 (1997).
29. J. Želudevičius, M. Mickus, and K. Regelskis, Opt. Express **26**, 27247 (2018).

FULL REFERENCES

1. J. D. Steinmeyer, C. L. Gilleland, C. Pardo-Martin, M. Angel, C. B. Rohde, M. A. Scott, and M. F. Yanik, "Construction of a femtosecond laser microsurgery system," Nat. Protoc. **5**, 395–407 (2010).
2. L. M. Haupert and G. J. Simpson, "Screening of protein crystallization trials by second order nonlinear optical imaging of chiral crystals (sonicc)," Methods **55**, 379 – 386 (2011).
3. H.-Y. Chung, R. Schubert, S.-H. Chia, S. Falke, C. N. Mudogo, F. X. Kärtner, G. Chang, C. Betzel *et al.*, "Protein-crystal detection with a compact multimodal multiphoton microscope," Commun. Biol. **3**, 1–7 (2020).
4. R. R. Gattass and E. Mazur, "Femtosecond laser micromachining in transparent materials," Nat. Photonics **2**, 219–225 (2008).
5. C. Xu and F. Wise, "Recent advances in fibre lasers for nonlinear microscopy," Nat. Photonics **7**, 875–882 (2013).
6. M. Piche, *Mode locking through nonlinear frequency broadening and spectral filtering*, vol. 2041 (SPIE, 1994).
7. K. Sun, M. Rochette, and L. R. Chen, "Output characterization of a self-pulsating and aperiodic optical fiber source based on cascaded regeneration," Opt. Express **17**, 10419–10432 (2009).
8. K. Regelskis, J. Želudevičius, K. Viskontas, and G. Račiukaitis, "Ytterbium-doped fiber ultrashort pulse generator based on self-phase modulation and alternating spectral filtering," Opt. Lett. **40**, 5255–5258 (2015).
9. D. Lin, D. Xu, J. He, Y. Feng, Z. Ren, and D. J. Richardson, "Generation of 625nj pulses from a mamyshev oscillator with a few-mode lma yb-doped fiber," in *2021 Conference on Lasers and Electro-Optics Europe and European Quantum Electronics Conference,* (Optical Society of America, 2021).
10. W. Liu, R. Liao, J. Zhao, J. Cui, Y. Song, C. Wang, and M. Hu, "Femtosecond mamyshev oscillator with 10-mw-level peak power," Optica **6**, 194–197 (2019).
11. E. Poeydebat, F. Scol, O. Vanvincq, G. Bouwmans, and E. Hugonnot, "All-fiber mamyshev oscillator with high average power and harmonic mode-locking," Opt. Lett. **45**, 1395–1398 (2020).
12. E. Poeydebat, F. Scol, O. Vanvincq, G. Bouwmans, and E. Hugonnot, "Pulse energy enhancement via filter shape optimization in an all-fiber mamyshev oscillator," in *Conference on Lasers and Electro-Optics,* (Optical Society of America, 2021), p. JTh3A.97.
13. B. Piechal, J. Szczepanek, T. M. Kardaś, and Y. Stepanenko, "Mamyshev oscillator with a widely tunable repetition rate," J. Light. Technol. **39**, 574–581 (2021).
14. T. Wang, B. Ren, C. Li, J. Wu, R. Su, P. Ma, Z.-C. Luo, and P. Zhou, "Over 80 nj sub-100 fs all-fiber mamyshev oscillator," IEEE J. Sel. Top. Quantum Electron. **27**, 1–5 (2021).
15. V. Boulanger, M. Olivier, F. Trépanier, M. Bernier, and M. Piché, "Efficient all-pm-fiber mamyshev oscillator based on fiber bragg gratings," in *Laser Congress 2020 (ASSL, LAC),* (Optical Society of America, 2020), p. JTu5A.6.
16. N. Tarasov, A. M. Perego, D. V. Churkin, K. Staliunas, and S. K. Turitsyn, "Mode-locking via dissipative faraday instability," Nat. Commun. **7** (2016).
17. A. M. Perego, "High-repetition-rate, multi-pulse all-normal-dispersion fiber laser," Opt. Lett. **42**, 3574–3577 (2017).
18. Z. Liu, Z. M. Ziegler, L. G. Wright, and F. W. Wise, "Megawatt peak power from a mamyshev oscillator," Optica **4**, 649–654 (2017).
19. I. Samartsev, A. Bordenyuk, and V. Gapontsev, "Environmentally stable seed source for high power ultrafast laser," in *Components and Packaging for Laser Systems III,* vol. 10085 A. L. Glebov and P. O. Leisher, eds., International Society for Optics and Photonics (SPIE, 2017), pp. 201 – 209.
20. Y.-H. Chen, P. Sidorenko, R. Thorne, and F. Wise, "Starting dynamics of a linear-cavity femtosecond mamyshev oscillator," J. Opt. Soc. Am. B **38**, 743–748 (2021).
21. P. Sidorenko, W. Fu, L. G. Wright, M. Olivier, and F. W. Wise, "Self-seeded, multi-megawatt, mamyshev oscillator," Opt. Lett. **43**, 2672–2675 (2018).
22. M. Pielach, B. Piechal, J. Szczepanek, P. Kabaciński, and Y. Stepanenko, "Energy scaling of an ultrafast all-pm-fiber laser oscillator," IEEE Access **8**, 145087–145091 (2020).
23. C. Aguergaray, N. G. R. Broderick, M. Erkintalo, J. S. Y. Chen, and V. Kruglov, "Mode-locked femtosecond all-normal all-pm yb-doped fiber laser using a nonlinear amplifying loop mirror," Opt. Express **20**, 10545–10551 (2012).
24. S. Pitois, C. Finot, L. Provost, and D. J. Richardson, "Generation of localized pulses from incoherent wave in optical fiber lines made of concatenated mamyshev regenerators," J. Opt. Soc. Am. B **25**, 1537–1547 (2008).
25. P. Sidorenko, W. Fu, and F. Wise, "Nonlinear ultrafast fiber amplifiers beyond the gain-narrowing limit," Optica **6**, 1328–1333 (2019).
26. G. P. Agrawal, *Nonlinear Fiber Optics* (Academic Press, 1995), 2nd ed.
27. S. K. Turitsyn, A. E. Bednyakova, M. P. Fedoruk, A. I. Latkin, A. A. Fotiadi, A. S. Kurkov, and E. Sholokhov, "Modeling of cw yb-doped fiber lasers with highly nonlinear cavity dynamics," Opt. Express **19**, 8394–8405 (2011).
28. R. Paschotta, J. Nilsson, A. Tropper, and D. Hanna, "Ytterbium-doped fiber amplifiers," IEEE J. Quantum Electron. **33**, 1049–1056 (1997).
29. J. Želudevičius, M. Mickus, and K. Regelskis, "Investigation of different configurations and operation regimes of fiber pulse generators based on nonlinear spectral re-shaping," Opt. Express **26**, 27247–27264 (2018).